13th ewtec 2019 Proceedings of the 13th European Wave and Tidal Energy Conference 1-6 Sept 2019, Naples, Italy

Optimal power take-off parameters for a bottom-hinged plate wave energy converter

Miguel Calvário, Josè F. Gaspar, Mojtaba Kamarlouei, and Carlos Guedes Soares

Abstract—**The objective of this paper is to derive the optimal parameters of an oil-hydraulic power take-off system for a bottom-hinged plate wave energy converter and to verify the impact of the state-of-the-art reactive control strategy on the converter performance. The power take-off concept relies on a concept of two-single rod oil-hydraulic cylinders working with a reciprocating movement on both sides of the bottom plate. The concept takes advantage of two possible hydraulic configurations to maximize their efficiency. The system is modelled with different controller's, whose parameters are optimized with genetic algorithms in order to maximize the harvested power. The mechanical interface between the power take-off and converter is also optimized considering technological constraints on the power take-off system and converter motions. The simulations are performed for different sea sate conditions.**

Keywords—**Bottom-hinged plate, Power take-off system, Oil-hydraulics, Wave energy converter.**

I. Introduction

WAVE energy converters (WECs) are devices designed to extract energy from waves, in which the harvested energy is converted into electrical one by means of a power take-off system (PTO). A wide range of concepts have been presented by academia and industry in the last decades, which includes oscillating water columns, point absorbers, terminators, attenuators and oscillating wave surge converters [1].

This paper covers the case of the bottom hinged-plate WEC, one kind of oscillating wave surge converter, made-off a buoyant plate hinged to the sea floor, in which the plate thickness is smaller than the other dimensions [2]. This WEC is installed in shallow waters and operates in pitch mode, moving back and forth with the surging movement of water particles close to the bottom [1]. Surface piercing and fully submerged prototypes were tested in open ocean, in case the Oyster [3] and Waveroller [4], using water and oil hydraulic PTO technologies, respectively.

This paper analyses a simplified surface piercing bottom-hinged plate bottom connected to a generic oil-hydraulic PTO system. The PTO [5] is based on the reciprocating movement of two cylinders, attached to both sides of the plate, in which the bi-directional oil power is sent to a hydraulic motor coupled with an electrical generator. The PTO allows two different oil-hydraulic cylinder configurations, one like a double-rod symmetric cylinder and other similar to a single rod cylinder, being possible to adjust pressure and force according to a specific sea state condition.

The objective of this paper is to analyse the performance of the PTO concept with two different oil-hydraulic configurations of a standard cylinder and comparing results using Proportional (P) and Proportional Integral (PI) controllers. The analysis is performed with constraints on the cylinder motion, in order to avoid excessive oscillations, and on the minimum average pressure of the double rod symmetrical cylinder. Both control and layout parameters are optimized with genetic algorithms.

This paper is organised in six sections. Section II presents the PTO Concept, while the modelling of WEC hydrodynamics and PTO system is presented in section III. In section IV the case study is developed, and the results analysis is presented in section V, being the paper summarized in the conclusions section.

II. PTO concept

The PTO consists of two single rod cylinders (c_1 and c_2 in Fig.1) hinged on both plate sides, oscillating with a

Paper ID number:1822- Conference track: GPC

This work was performed within the Strategic Research Plan of the Centre for Marine Technology and Ocean Engineering, which is financed by Portuguese Foundation for Science and Technology (FCT), the project "Generic hydraulic power take-off system for wave energy converters" funded by FCT under contract PTDC/EMS-SIS-1145/2014 and the project "Experimental simulation of oil-hydraulic Power Take-Off systems for Wave Energy Converters", funded by FCT under contract PTDC/EME-REN/29044/2017.

M. Calvário is a Researcher Assistant at the Centre for Marine Technology and Ocean Engineering (CENTEC), Instituto Superior Técnico, Universidade de Lisboa, Av. Rovisco Pais, 1049-001 Portugal (e-mail: miguel.calvario@centec.tecnico.ulisboa.pt).

J. F. Gaspar is a PhD Researcher at CENTEC, Instituto Superior Técnico, Universidade de Lisboa, Av. Rovisco Pais, 1049-001 Portugal (e-mail: jose.gaspar@centec.tecnico.ulisboa.pt).

M. Kamarlouei is a Researcher Assistant at the Centre for Marine Technology and Ocean Engineering (CENTEC), Instituto Superior Técnico, Universidade de Lisboa, Av. Rovisco Pais, 1049-001 Portugal (e-mail: mojtaba.kamarlouei@centec.tecnico.ulisboa.pt).

C. Guedes Soares is a Distinguished Professor and President of the Centre for Marine Technology and Ocean Engineering (CENTEC), Instituto Superior Técnico, Universidade de Lisboa, Av. Rovisco Pais, 1049-001 Portugal (e-mail: c.guedes.soares@centec.tecnico.ulisboa.pt).

surging movement [3], [6]. The layout of the attachment is symmetrical in relation to the vertical axis, being this concept based on a third-class lever mechanism [5], [7]. In addition, two or more rows of cylinders can be added in parallel, in order to maximize the harvested power.

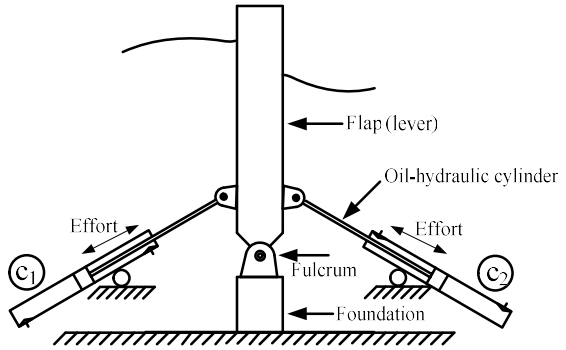

Fig. 1. Oscillating wave surge converter with a reciprocating PTO concept. Adapted from [5] and [8]-[11].

The PTO working principle is based on a reciprocating movement of cylinders, allowing two different oil-hydraulic configurations, PTO A and PTO B The configuration of PTO A, is similar to a double rod symmetric cylinder, in which the rodless chambers are linked by a direct connection (ports e and f, Fig.2) and annular chambers are linked to the pump. On the other hand, in PTO B the rodless chambers are connected to the pump while the annular chambers are connected directly. As the cylinders move in opposite directions, the total oil volume displacement between the chambers is the same [12].

For instance, in case of PTO configuration A when the plate rotates clockwise the oil inside cylinder c1 (Fig. 2) is compressed and the cylinder moves upwards producing power, while cylinder c2 (Fig. 2) is in idle mode, moving downwards. This cylinder will produce power during the plate counterclockwise rotation while cylinder c1 will be in the idle mode.

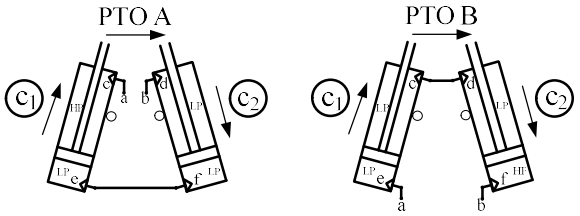

Fig. 2. PTO reciprocating concept. Adapted from [5], [12].

PTO configuration A is suitable for low energetic sea state conditions, because the oil pressure can be increased in order to maintain the pump and other hydraulic component at a reasonable efficiency level [13]. On the other hand, configuration B is suitable for more energetic sea states, taking advantage of a higher buckling force.

III. MODELLING

This section outlines the hydrodynamic modelling of the WEC and the PTO system.

A. Hydrodynamics

The WEC is modelled, according to the diagram presented in Fig.3, with the linear potential theory and methodologies presented in the literature [2], [14]. The interaction between waves and the WEC is given by:

$$J_s\ddot{\theta}(t) = M_e(t) + M_h(t) + M_r(t) + M_{PTO}(t) \quad (1)$$

where J_s is the inertia mass moment relative to the fulcrum axis, $\ddot{\theta}(t)$ is the plate angular acceleration, M_e is the moment of excitation, M_h is the hydrostatic moment, M_r is the radiation moment and M_{PTO} is the moment produced by the PTO system.

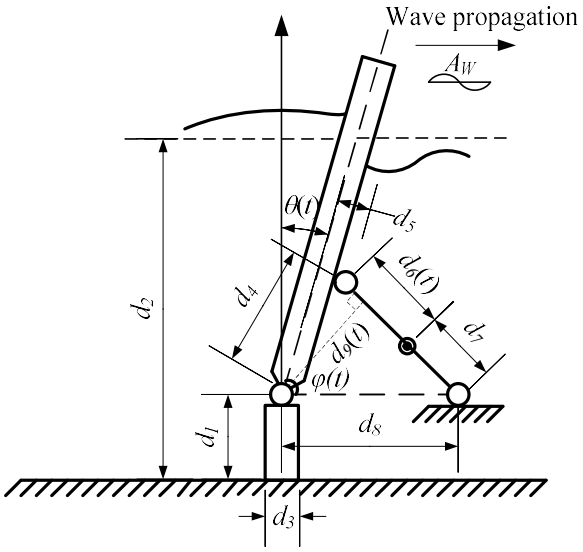

Fig. 3. WEC geometrical parameters (not in scale). Adapted from [5], [6] and [15].

The development of (1) in time domain, without considering fluid viscous effects, results in [2]:

$$[J_s + A_\infty]\ddot{\theta}(t) + \int_0^t k_r(t-\tau)\,\dot{\theta}(\tau) + k_h\theta(t) = M_e(t) + M_{PTO}(t) \quad (2)$$

where A_∞ is the added moment of inertia at infinite frequency, k_h is the hydrostatic restoring coefficient and k_r is the radiation impulse response function.

The values of k_h and k_r are given respectively with [2]:

$$k_h = \rho g V_p r_b - m_p g r_g \quad (3)$$

$$k_r(t) = \frac{2}{\pi}\int_0^t B(\omega)\cos(\omega t)\,d\omega \quad (4)$$

where ρ is the water density, g is the gravity acceleration, V_p is the displaced volume, r_b is the distance between the fulcrum axis and the centre of buoyancy, m_p is the mass of the plate, r_g is the distance between the fulcrum axis and centre of gravity, $B(\omega)$ is the radiation damping coefficient and ω is the wave angular frequency.

The moment of excitation is [2]:

$$M_{ext}(t) = \sum_{n=1}^{N} A_{w,n}(\omega_n)\,|\Gamma(\omega_n)|\cos\big(-\omega_n t + \varphi_n + \angle\Gamma(\omega_n)\big) \quad (5)$$

where n is the index of wave component, $A_{w,n}$ is the wave amplitude, $|\Gamma(\omega_n)|$ is the excitation moment amplitude, φ_n are random phases, $\angle\Gamma(\omega_n)$ is the excitation phase difference and N is the number of frequencies.

The value of $A_{w,n}$ is obtained with:

$$A_{w,n} = \sqrt{2S(\omega_n)\Delta\omega} \quad (6)$$

where $S(\omega_n)$ is the energy density spectrum while $\Delta\omega$ is the difference between two consecutive frequencies.

In the present study, the Pierson-Moskowitz formulation is used [16], described by:

$$S(\omega_n) = 5\pi^4 \frac{{H_s}^2}{{T_P}^4}\frac{1}{{\omega_n}^5}\exp\left[\frac{-20\pi^4}{{T_P}^4}\frac{1}{{\omega_n}^4}\right] \quad (7)$$

where T_p and H_s are the peak wave period and the significant wave height, respectively.

B. Power take-off system

The PTO is analysed without considering the modelling of the pumps and the high pressure pipeline. It is assumed an ideal PTO in which the cylinder harvested power is described as:

$$P_c(t) = F_c(t)\dot{d}_6(t) = \frac{M_{PTO}(t)\dot{d}_6(t)}{d_9(t)} \quad (8)$$

where F_c is force on the cylinder, $d_6(t)$ is the displacement of the cylinder, and $d_9(t)$ is the moment arm.

The PTO force and moment are described as [2], [17]:

$$F_{PTO}(t) = \frac{M_{PTO,ref}(t)}{l_9(t)} \quad (9)$$

$$M_{PTO}(t) = K_C\theta(t) + B_C\dot{\theta}(t) \quad (10)$$

where K_C (spring) and B_C (damping) are the PTO control parameters.

The cylinder buckling force, which should not be exceed is obtained with [18]:

$$F_{PTO}(t) \le F_{buckling} = \frac{\pi^2 EI}{v{d_k}^2} \quad (11)$$

where E is the modulus of elasticity, I is the geometrical inertia moment of the cylinder rod cross section, v is the safety factor and d_k is the free buckling length.

The geometrical parameters $d_6(t)$, $d_8(t)$, $d_9(t)$ and $\varphi(t)$ are obtained with [5]:

$$d_6(t) = -d_7 + \sqrt{{d_4}^2 + {d_8}^2 - 2d_4 d_8\cos\big(\varphi(t)\big)} \quad (12)$$

$$d_9(t) = \frac{d_4 d_8\sin\big(\varphi(t)\big)}{d_6(t) + d_7} \quad (13)$$

$$\varphi(t) = \varphi_0 - \theta(t) \quad (14)$$

$$\varphi_0 = \frac{\pi}{2} - \sin^{-1}\left(\frac{d_5}{d_4}\right) \quad (15)$$

$${d_8}^2 - (2d_4\cos(\varphi_0))d_8 + {d_4}^2 - \big(d_{6,0} + d\big)^2 = 0 \quad (16)$$

where $d_{6,0}$ is the cylinder initial position and d_5 is the distance between the cylinder rod and plate middle axis.

The cylinder average pressure and power are determined with [19]:

$$\bar{p_c} = \frac{4F_c}{\pi\big({d_p}^2 - {d_r}^2\big)} \quad (17)$$

$$\bar{P_c} = \frac{1}{t_f - t_i}\int_{t_i}^{t_f} F_c\dot{d}_6(t)\,dt \quad (18)$$

where d_p and d_r are the cylinder piston and rod diameters respectively.

IV. CASE STUDY

This section presents the WEC modelling main parameters and assumptions. The plate hydrodynamic coefficients $A(\omega)$, $B(\omega)$ and $\Gamma(\omega)$ are determined with the Nemoh software [20]. The plate is modelled as a rectangular box with a length of 8.4 (m), width of 18 (m) and thickness of 1.8 (m), and hinged to a foundation (d_1=3 m) by means of a triangular downwards structure (1 m height). The modelling approach is adapted from [21]. The behaviour of the hydrodynamic coefficients against the wave period is presented in Fig.4 and the sea state conditions (H_s and T_p) are presented in Table I.

TABLE I
SEA STATE CONDITIONS [5].

SS	H_s (m)	T_p (s)
1	0.75	5.45
2	1.25	5.98
3	1.75	6.59
4	2.25	7.22
5	2.75	7.78

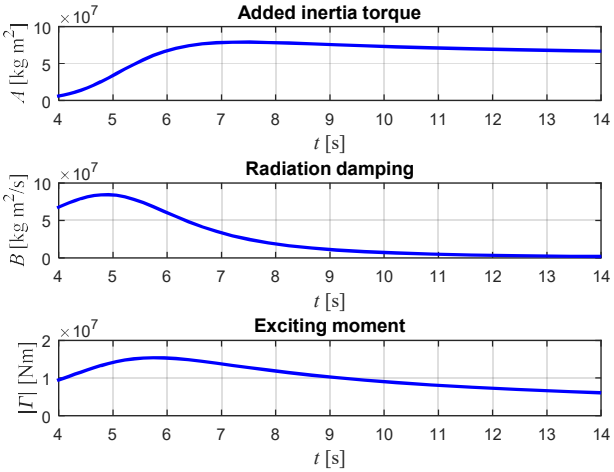

Fig. 4. Hydrodynamic coefficients $A(\omega)$, $B(\omega)$ and $\Gamma(\omega)$ versus the wave period [5].

The k_r parameter is obtained in the frequency domain ($K_r(i\omega)$), in order to avoid solving the convolution integral of the radiation IRF (4), with the following expressions, [22]:

$$K_r(i\omega) = -\mathrm{B}(\omega) + i\omega(A(\omega) - A_\infty) \tag{29}$$

$$\widehat{K}_r(\mathrm{s}) = \frac{c_m s^m + c_{m-1}s^{m-1} + \cdots + c_0}{di_m s^m + di_{m-1}s^{m-1} + \cdots + di_0} \tag{20}$$

where $\widehat{K}_r(\mathrm{s})$ is a rational transfer function that is used to perform an approximation of $K_r(i\omega)$.

A fifth order approximation was set, using an open source toolbox [23], and the collected results (after the transformation to time domain, $k(t)$) are presented in Fig. 5.

A mill type standard cylinder [18] with a piston diameter of 320 (mm) and rod of 200 (mm) is used with a maximum working pressure up to 350 (bar). The distance d_7 is set in to minimize the distance between the trunnion position and the cylinder clevis, in order to increase the buckling force. The WEC hydrodynamic and PTO parameters are presented in Table II.

An optimization procedure is undertaken, in order to maximize the harvested power (objective function), considering a maximum and minimum plate pitching angle (θ_{max}, θ_{min}) and a minimum average pressure ($\bar{p}_{cmin}$) The problem is defined as [5], [24]:

$$min\left[-\left(\frac{1}{T}\int_0^T P_c(t)dt\right) + \sum_{i=1}^{m} C_i {d_i}^{k_1}\right] \tag{21}$$

$$g_1(d_4, K_C, B_C) = \bar{p}_{cmin} - \bar{p}_c \leq 0 \tag{22}$$

$$g_2(d_4, K_C, B_C) = \theta_{min} - \min(\theta) \leq 0 \tag{23}$$

TABLE II
HYDRODYNAMIC AND PTO PARAMETERS [5].

Symbol	Value	Unit
ρ	1025	$k_g\,m^{-3}$
g	9.806	$m\,s^{-2}$
V_p	288.36	m^3
r_b, r_g	4.945	m
m_p	$98.523\text{x}10^3$	k_g
C	$9.555\text{x}10^6$	N m
J_s	$2.713\text{x}10^6$	$k_g\,m^2$
J_∞	$2.12\text{x}10^7$	$k_g\,m^2$
$[c_4,\ldots,c_0]$	*(1)	---
$[di_4,\ldots,di_0]$	*(2)	---
$F_{sat\ piston}$	281.5	Ton
$F_{sat\ ring}$	148.4	Ton
d_1	3	m
d_5	1.4	m

*(1) [1.003 1.009 4.612 3.574]x10⁸
*(2) [1. 2.585 7.736 13.388 12.788 9.6974]

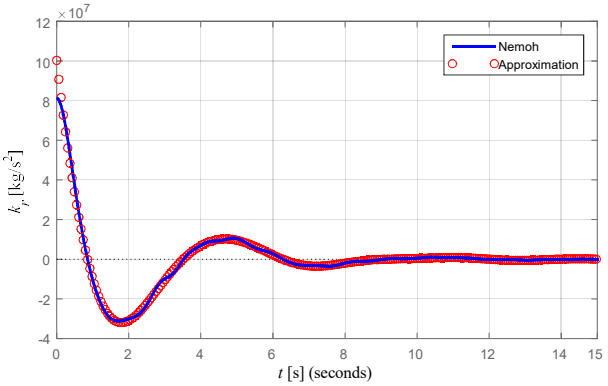

Fig. 5. Radiation IRF $k_r(t)$ and approximated value [5].

$$g_3(d_4, K_C, B_C) = max(\theta) - \theta_{max} \leq 0 \tag{24}$$

The decision variables are the control parameters (K_C, B_C) and the distance d_4. The latter is constrained between 2 and 2.2 (m) and control parameters to $K_C \in [-1\text{x}10^6, 1\text{x}10^9]$ and $B_C \in [0.1\text{x}10^6, 1\text{x}10^9]$. These bounds are based on previous studies regarding reactive control of points absorbers WECs [17].

The value of $\bar{p}_{cmin}$ is defined as 170 (bar) in order to avoid losses on hydraulic components (e.g. pump [13]) and the angle is limited to 30 (º) based on the assumption of linear wave theory [2]. The optimal parameters are obtained with genetic algorithms following the method presented in [5] and [19]. The optimization is performed with a population of 200 individuals and 25 generations.

The optimization process is performed with two scenarios (S1 and S2) as follows:

S1 - Two rows of cylinders are modelled considering the oil pressure constraint and using the PTO A configuration;

S2 - Two rows of cylinders are modelled with the PTO configuration B although with no pressure constraint.

P and PI controllers are studied, in both scenarios, in order to determine their impact on the harvested power.

V. RESULTS

The results as regards the harvested power ($\bar{P}_c$), maximum and minimum power peaks ($\max(P_c)$, $\min(P_c)$, respectively) ratio between maximum peaks and average power ($\max(P_c)/\bar{P}_c$) and ratio between minimum and maximum power peaks ($\min(P_c) / \max(P_c)$) are presented in Table III.

As revealed in Table III, $\bar{P}_c$ increases with the sea state energetic condition in both PTO configurations and control approaches. Moreover, higher values of $\bar{P}_c$ are achieved by using PTO configuration B (scenario S2) with both controllers and in all sea state conditions. PTO configuration B takes advantage of a higher buckling force and, since the pressure is not constrained, a larger value of harvested power is obtained. PTO configuration A is more likely to have a higher efficiency in the less energetic conditions because the oil pressure fluctuates around 170 (bar) with impact on pump efficiency, and so may be implemented in such conditions.

TABLE III
CYLINDER AVERAGE AND PEAK HYDRAULIC POWER FOR SCENARIOS S1 AND S2

	Controller				
		P		PI	
	SS	S1	S2	S1	S2
$\bar{P}_c$ [kW]	1	---	8.8	---	9.7
	2	20.2	25.6	25.9	29.1
	3	51.4	52.6	58.6	61.7
	4	81.9	89.9	91.4	107.1
	5	119.4	132.9	134.3	173.6
$\max(P_c)$[kW]	1	---	74	---	87.4
	2	331.8	317	361.1	412.1
	3	337.2	332.3	384.3	434.6
	4	724.88	1013.2	799.6	1171.5
	5	821.3	1086.1	912.3	1399.9
$\min(P_c)$ [kW]	1	0	0	---	-7.3
	2	0	0	-301.1	-37.6
	3	0	0	-120.8	-37.8
	4	0	0	-345.4	-244.8
	5	0	0	-456	-476.2
$\max(P_c)/\bar{P}_c$	1	---	8.4	---	9
	2	16.4	12.4	13.9	14.2
	3	6.6	6.3	6.6	7
	4	8.9	11.3	8.7	10.9
	5	6.9	8.2	6.8	8.1
$\left\lvert\frac{\min(P_c)}{\max(P_c)}\right\rvert$	1	---	---	---	0.1
	2	---	---	0.8	0.1
	3	---	---	0.3	0.1
	4	---	---	0.4	0.2
	5	---	---	0.5	0.3

The results reveal higher values of harvested power ($\bar{P}_c$) obtained with a PI control in both scenarios, mostly on scenario S2, where it increases with the sea energetic level. A similar behaviour is also observed for $\max(P_c)$, except for SS4 and SS5 conditions.

The minimum power peaks $\min(P_c)$ are negative using a PI controller, meaning that the PTO should reverse some energy during the oscillation cycle in order to perform the reactive control [25]. In contrast, minimum power peaks are null with a P controller, thus not requiring reactive energy.

In case of $\max(P_c)/\bar{P}_c$, higher values are reached in SS2 condition, for both controllers and scenarios, being the difference among scenarios meaningful with the P controller approach (16.4 and 12.4 ratios in scenarios S1 and S2 respectively). The 16.4 ratio indicates that the maximum peak power is more than sixteen times of the average one, thus with more demand on the PTO storage capacity and components. As a result, the PTO will be designed to operate at extreme but less frequent conditions, and then, at non-optimal conditions most of the time. This problem may be minimized with a trade-off on the sizing of the PTO components (e.g. pumps, accumulators, [19]). As regards to the $|\min(P_c) / \max(P_c)|$ ratio, it varies between 0.3 and 0.8 in scenario S1 and between 0.1 and 0.3 in scenario S2.

According to the results the reactive control (PI) approach is the most appropriate to increase the power harvesting performance, however using a P controller approach is more likely to contribute for a higher PTO efficiency, because there is no need to reverse hydraulic energy during small periods of the working cycle. For instance, the required reactive power of 476.2 kW, with PTO configuration B in SS5 condition, requires the use of large displacement pump (e.g. 750 (cm^3) [26]) or, in alternative, a tandem assembly of smaller pumps, which may have a positive impact on the PTO overall efficiency. Thus, further research is required in order to evaluate the PTO efficiency using a P controller with this WEC concept and using a PTO technology based on the reciprocating movement of single rod cylinders.

VI. CONCLUSIONS

The simulation results indicate that the "single-rod cylinder" configuration is suitable for an increment on the harvested power with the proposed PTO, mostly when using a PI control approach. However, the PTO efficiency was not considered in these simulations, which in case of a P control approach is expected to be higher than in the PI one, since there is no need to use reactive energy and bigger components.

REFERENCES

[1] C. Guedes Soares, J. Bhattacharjee, M. Tello, and L. Pietra, "Review and classification of wave energy converters," in *Maritime Engineering and Technology*, C. Guedes Soares, Y. Garbatov, S. Sutulo, and T. A. Santos, Eds. London: Taylor & Francis Group, 2012, pp. 585–594.

[2] R. P. F. Gomes, M. F. P. Lopes, J. C. C. Henriques, L. M. C. Gato, and A. F. O. Falcão, "The dynamics and power extraction of bottom-hinged plate wave energy converters in regular and irregular waves," *Ocean Eng.*, vol. 96, no. 1, pp. 86–99, 2015.

[3] E. Renzi, K. Doherty, A. Henry, and F. Dias, "How does Oyster work ? The simple interpretation of Oyster mathematics," *Eur. J. Mech. B / Fluids*, vol. 47, pp. 124–131, 2014.

[4] J. Lucas, M. Livingstone, M. Vuorinen, and J. Cruz, "Development of a wave energy converter (WEC) design tool – application to the WaveRoller WEC including validation of numerical estimates," in *4th International Conference on Ocean Energy*, 2012.

[5] M. Calvário, J. F. Gaspar, M. Kamarlouei, T. S. Hallk, and C. Guedes Soares, "Oil-hydraulic power take-off concept for a bottom-hinged plate wave energy converter. Submitted to publication.

[6] E. Renzi and F. Dias, "Hydrodynamics of the oscillating wave surge converter in the open ocean," *Eur. J. Mech. B/Fluids*, vol. 41, pp. 1–10, 2013.

[7] M. Calvário, J. F. Gaspar, and C. Guedes Soares, "Comparative study of lever mechanisms connected to oil-hydraulic power take-off systems," in *Renewable Energies Offshore*, C. Guedes Soares, Ed. London: Taylor & Francis Group, 2015, pp. 271–278.

[8] D. Zhang, W. Li, Y. Ying, H. Zhao, Y. Lin, and J. Bao, "Wave energy converter of inverse pendulum with double action power take off," *Proc. Inst. Mech. Eng. Part C J. Mech. Eng. Sci.*, vol. 227, pp. 2416–2427, 2013.

[9] Y. G. Lin, L. Tu, D. H. Zhang, H. W. Liu, and W. Li, "A study on dual-stroke pendulum wave energy conversion technology based on a water / oil integrated transmission system," *Ocean Eng.*, vol. 67, pp. 27–34, 2013.

[10] D. Zhang, W. Li, Y. Lin, and J. Bao, "An overview of hydraulic systems in wave energy application in China," *Renew. Sustain. Energy Rev.*, vol. 16, pp. 4522–4526, 2012.

[11] P. Schmitt, C. Windt, J. Nicholson, and B. Elsässer, "Development and validation of a procedure for numerical vibration analysis of an oscillating wave surge converter," *Eur. J. Mech. B / Fluids*, vol. 58, pp. 9–19, 2016.

[12] J. F. Gaspar, A. Sinha, M. Calvário and C. Guedes Soares, "Concept of reciprocating oil-hydraulic cylinders for increased wave power harvesting," in *Progress in Renewable Energies Offshore*, C. Guedes Soares, Ed. London, U.K.: Taylor & Francis Group, 2016, pp. 463-471.

[13] J. F. Gaspar, M. Calvário, M. Kamarlouei, and C. Guedes Soares, "Power-take-off concept for wave energy converters based on oil-hydraulic transformer units," *Renew. Energy*, vol. 86, pp. 1232–1246, 2016.

[14] N. T. Bozo, D. Karmakar, and C. Guedes Soares, "Numerical investigation of a submerged surging plate wave energy converter," in *Renewable Energies Offshore*, C. Guedes Soares, Ed. London: Taylor & Francis Group, 2015, pp. 515–522.

[15] D. Sarkar, K. Doherty, and F. Dias, "The modular concept of the Oscillating Wave Surge Converter," *Renew. Energy*, vol. 85, pp. 484–497, 2016.

[16] Z. Y. Tay and V. Venugopal, "Hydrodynamic interactions of oscillating wave surge converters in an array under random sea state," *Ocean Eng.*, vol. 145, pp. 382–394, 2017.

[17] R. H. Hansen, M. M. Kramer, and E. Vidal, "Discrete Displacement Hydraulic Power Take-off System for the Wavestar Wave Energy Converter," *Energies*, vol. 6, pp. 4001–4044, 2013.

[18] Bosch Rexroth AG, "Hydraulic cylinder mill type, Series CDH3 / CGH3 / CSH3 RE 17338/07.13," 2013.

[19] J. F. Gaspar, M. Calvário, M. Kamarlouei, and C. Guedes Soares, "Design tradeoffs of an oil-hydraulic power take-off for wave energy converters," *Renew. Energy*, vol. 129, pp. 245–259, 2018.

[20] A. Babarit and G. Delhommeau, "Theoretical and numerical aspects of the open source BEM solver NEMOH," *in 11th European Wave and Tidal Energy Conference (EWTEC2015)*, 2015.

[21] L. Cameron et al., "Design of the Next Generation of the Oyster Wave Energy Converter," i*n 3rd International Conference on Ocean Energy (ICOE)*, 2010, pp. 1–12.

[22] A. Roessling and J. V. Ringwood, "Finite order approximations to radiation forces for wave energy applications," *in Renewable Energies Offshore*, C. Guedes Soares, Ed. London: Taylor & Francis Group, 2015, pp. 359–366.

[23] T. Perez and T. I. Fossen, "A Matlab Toolbox for Parametric Identification of Radiation-Force Models of Ships and Offshore Structures," *Model. Identif. Control. MIC*, vol. 30, no. 1, pp. 1–15, 2009.

[24] T. Bäck, D. B. Fogel, and Z. Michalewicz, *Handbook of Evolutionary Computation*. New York: Oxford, 1997.

[25] J. Falnes, "Optimum Control of Oscillation of Wave-Energy Converters", *in 11th International Offshore and Polar Engineering Conference*, 2001, pp. 567-574.

[26] Bosch Rexroth AG, "Axial Piston Variable Pump A4VSG Series 1x and 3x," 2018.